TÜBİTAK

Turkish Journal of Chemistry

http://journals.tubitak.gov.tr/chem/

Research Article

Turk J Chem
(2019) 43: 1159 – 1169
© TÜBİTAK
doi:10.3906/kim-1903-32

Molecular dynamics simulations of adsorption of long pyrene-PEG chains on a thin carbon nanotube

Pelin Deniz AKKUŞ, Ayşe Özge KÜRKÇÜOĞLU LEVİTAS*
Department of Chemical Engineering, Faculty of Engineering, İstanbul Technical University, İstanbul, Turkey

Received: 09.03.2019 • **Accepted/Published Online:** 14.06.2019 • **Final Version:** 06.08.2019

Abstract: Carbon nanotubes have emerged as highly promising theranostic agents due to their unique structural/physical features, high surface area, and high drug-loading capacity. The high cytotoxicity of carbon nanotubes can be eliminated by noncovalent coating using hydrophilic polymers. We investigated the adsorption of long pyrene functionalized polyethylene glycol (PEG) chains, PEG_{2000} and PEG_{5000}, on a single-walled carbon nanotube (SWNT) from a crowded solution. Full-atom molecular dynamics simulations in explicit water were used to mimic the experimental conditions of noncovalent PEGylation with a stoichiometry of one SWNT to ten pyrene-PEG. Although the diffusional behavior of the pyrene molecules still attached to the polymers did not change according to chain length, the adsorption rate for pyrene-PEG_{2000} to the SWNT was higher than that for pyrene-PEG_{5000} chains. Here longer chains sterically hindered the adsorption of pyrene groups on the SWNT surface. Once adsorbed, pyrene molecules stayed on the SWNT surface even though they frequently adopted different orientations that may weaken their $\pi - \pi$ stacking interactions with the nanotube surface.

Key words: Adsorption, interaction energy, PEGylation, controlled drug delivery

1. Introduction

Carbon nanotubes (CNTs) have been examined in terms of biomedical applications due to their numerous chemical and physical properties, such as high aspect ratios, large surface areas, rich surface chemical functionalities, and size stability at nanoscale [1–5]. While the cytotoxicity of CNTs mostly depends on their concentration [6], the most significant obstacle to their biomedical applications is their tendency to form bundles in aqueous environments [7]. In order to overcome this limitation while maintaining the desirable properties of CNTs, noncovalent conjugation with hydrophilic polymeric chains, such as with polyethylene glycol (PEG), is an ideal approach [8–10]. For drug-carrying purposes, noncovalent coating of PEG on CNTs can increase their solubility and extend their circulating times in blood [5]. The solubility of these nanocarriers can be improved by studying nonbonded molecular interactions between the CNT and its coating controlling the performance of the complex at macroscopic scale.

Noncovalent conjugation of CNTs by polymeric chains is basically an adsorption process driven by nonbonded interactions between atoms. In the adsorption phenomena, properties of the solid surface, adsorbate, and solvent significantly affect the stability of these interactions. Molecular dynamics (MD) simulations enable one to study the effect of each parameter on adsorption, which in turn can provide useful insights into the stability of the CNT–polymer complex during biomedical applications [11]. So far, MD simulations indicated

*Correspondence: olevitas@itu.edu.tr

that the CNT diameter [12] and chirality [13] have a significant impact on polymer–CNT interactions. On the other hand, solvent polarity was shown to affect polymer adsorption on CNTs by altering polymer flexibility and the strength of nonbonded interactions [14]. MD simulations also provided important details on the interaction between CNTs and various polymeric systems, such as pyrene-attached polyethylene chains [14], branched PPO–polyethylene oxide segments [15], different polyether surfactants [16], polyamide-66 [17], lipid-PEG chains [18], and different flexible polymers [19,20].

CNTs are basically graphitic surfaces rolled up along different directions. The angle and direction of the rolling result in CNTs with surfaces having different aromaticity patterns decorated with a network of sp^2 carbon atoms [21–24]. This property secures numerous possibilities for the noncovalent functionalization of CNTs such as by using aromatic molecules [25] like pyrene. Pyrene molecules were shown to interact with CNTs through $\pi - \pi$ stacking interactions [26–31]. This π-stacking is strong enough to tether long flexible polymer chains on the CNT sidewall [14,32] as well as to immobilize proteins [33]. For biomedical applications, the noncovalent attachment of pyrene-polymer chains on CNTs can provide good solubility in aqueous environments and low cytotoxicity [32].

Various computational studies revealed that once attached to the nanotube surface, hydrophilic polymers, such as PEG can extend to the solvent side and provide an invisibility cloak to the nanotube for a long time [18,34]. In vitro stability, i.e. low cytotoxicity of these complexes, was recently reported by our group [32]. However, detailed transport properties and conformational dynamics of pyrene-PEG chains and CNT systems in a crowded solution, as in experimental conditions, remain elusive. Understanding these properties is of paramount importance for controlling the adsorption phenomena in these systems. In a previous study [32], pyrene-PEG chain size, single-walled CNT size, and stoichiometric ratio of single-walled CNTs to pyrene-PEG chains were shown to affect the noncovalent coating of nanotubes using computational and experimental techniques. Different from the previous study, here we studied and reported in detail the adsorption phenomena of long pyrene-PEG chains on a single-walled CNT in a concentrated aqueous solution. The focus was on the effect of chain molecular weight on their adsorption rate over a CNT surface using full-atom MD simulations. In addition, diffusional behaviors of both adsorbed and free pyrene molecules attached to long PEG chains were analyzed. The dynamics of PEG chains were also investigated to reveal their effect on the adsorption process. Finally, the interaction energies of pyrene-PEG chains of two different molecular weights on the CNT wall were calculated using an efficient configurational sampling approach.

2. Results and discussion

2.1. Adsorption of pyrene-PEG chains on a single-wall carbon nanotube

Figure 1 displays the time evolution of distances between the pyrene ends and central axis of the single-wall carbon nanotube (SWNT). When the pyrene end of a PEG chain was next to the SWNT, it spontaneously adsorbed on its surface. Interactions between these aromatic groups were stabilized by strong $\pi - \pi$ stacking interactions. All adsorbed pyrene-PEG chains stayed on the SWNT surface during the simulations (Figure 1). Interestingly, adsorbed pyrene molecules adopted different orientations, such as in parallel and perpendicular to the nanotube surface or nanotube end. For this reason, distances between the pyrene and axis of the SWNT changed between 3.3 Å (in SWNT entrance) and 10.4 Å (in perpendicular orientation). Here the adsorption distance between the pyrene group and SWNT surface was $\sim$3.6 Å, which agreed well with the adsorption distance of pyrene-polyethylene chains on a thin SWNT (3.6 Å) [14] and on flat graphene (3.5 Å) [35].

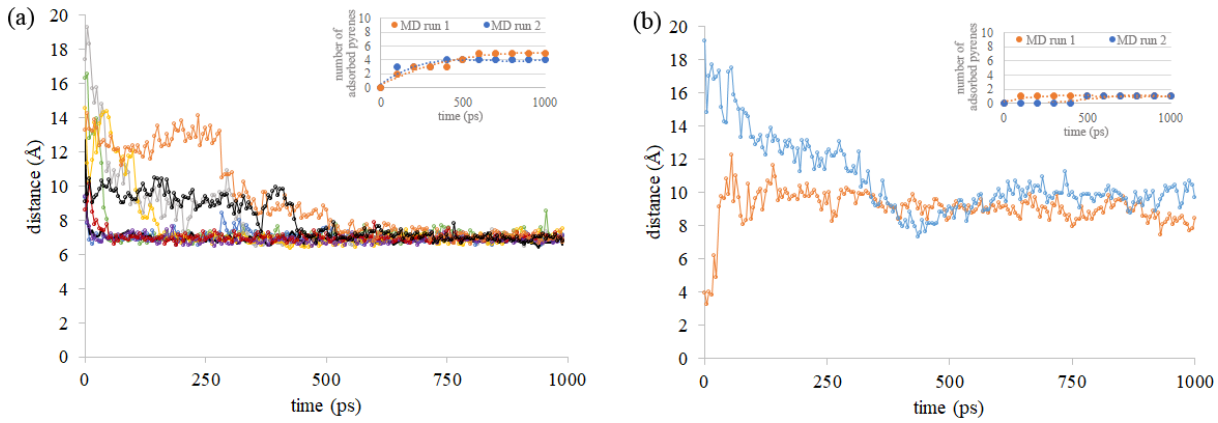

Figure 1. Evolution of distance between adsorbed pyrene molecules and SWNT for (a) Model-1, (b) Model-2. MD run 1 and MD run 2 indicate independent runs for each model.

In both independent simulations of duration 1 ns, four to five out of ten freely diffusing pyrene-PEG_{2000} chains were adsorbed on the thin SWNT surface (Figure 1a, inset). However, only one pyrene-PEG_{5000} chain out of ten chains was able to adsorb (Figure 1b, inset). The reason behind the low number of adsorbed pyrene-PEG_{5000} chains was the occupation of the nanotube surface by long flexible PEG chains due to van der Waals interactions [36]. Steric hindrance for the pyrene adsorption on the SWNT built up with longer PEG chains.

Figure 2 displays the time evolution of angles between the vectors normal to the pyrene surface and to SWNT pores throughout the trajectory. Accordingly, an angle of 90° indicated that the position of the pyrene molecules was parallel to the nanotube surface, the most energetically stable orientation, as will be discussed for interaction energy calculations. Angle evolutions verified that pyrene adsorbed on the SWNT surface in parallel and stayed in this orientation while diffusing on the nanotube surface. The pyrene end of longer PEG_{5000} chains bound in perpendicular orientation to the surface (Figure 2, last row). Even in this position, the pyrene molecules did not desorb from the surface, as Figure 1b also indicates. The length and flexibility of PEG chains did not detach the pyrene from the SWNT sidewall; therefore, the chain length seemed not to affect the adsorption of the pyrene molecules.

Once adsorbed, all pyrene molecules laterally diffused on the curved SWNT without detaching (see Figure 1), as was previously observed for similar systems [14]. Time average mean squared displacement (MSD) was calculated to investigate the spread of adsorbed pyrene motions on the SWNT surface and in the solution (Figure 3). Here pyrene-PEG chains in solution will be referred to as 'free' as well. When the diffusion of the pyrene ends of short (Figure 3a) and long polymer chains (Figure 3b) in solution was compared, the average MSD trends were similar, as expected for high polymer concentrations [37]. Figure 3c indicates that some adsorbed pyrenes attached to PEG_{2000} had lower MSD values, which implied that they experienced viscous forces more. The diffusional behavior of the pyrene molecules seemed to reflect the local packing on the nanotube surface, which constantly changed due to diffusion of pyrene molecules and coiling of PEG chains. The extent of unconstraint motion of adsorbed chains (Figure 3c) was similar to pyrene-PEG motions in the solution (Figure 3a), attaining MSDs $\sim$100 $Å^2$ at 1 ns. Interestingly, pyrene motions while attached to PEG_{5000} had similar MSD trends when adsorbed and free in solution (Figures 3b and 3d). This suggested that pyrene ends could diffuse to the same extent when adsorbed and free in solution, if the SWNT sidewall is not fully covered.

On the other hand, the spread of adsorbed pyrene-PEG_{5000} (Figure 3d) was similar to the adsorbed

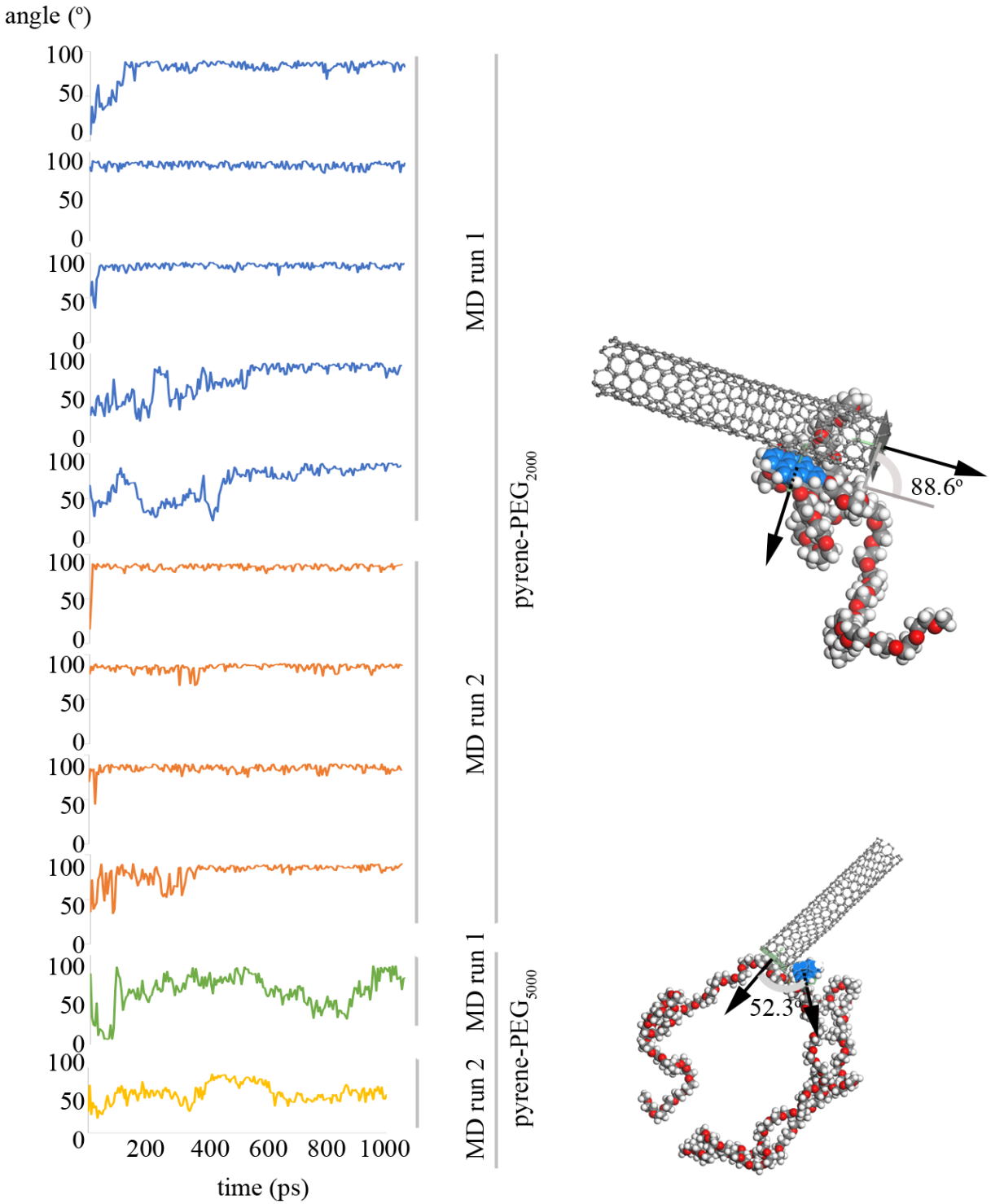

Figure 2. Angle evolution for absorbed pyrene-PEG chains in Model-1 and Model-2.

pyrene-PEG_{2000} experiencing less viscous forces (Figure 3c). Here it was difficult to differentiate the effect of chain length on the diffusional behavior of adsorbed pyrene ends. The surface coverages on SWNT in short and long chain systems were not similar.

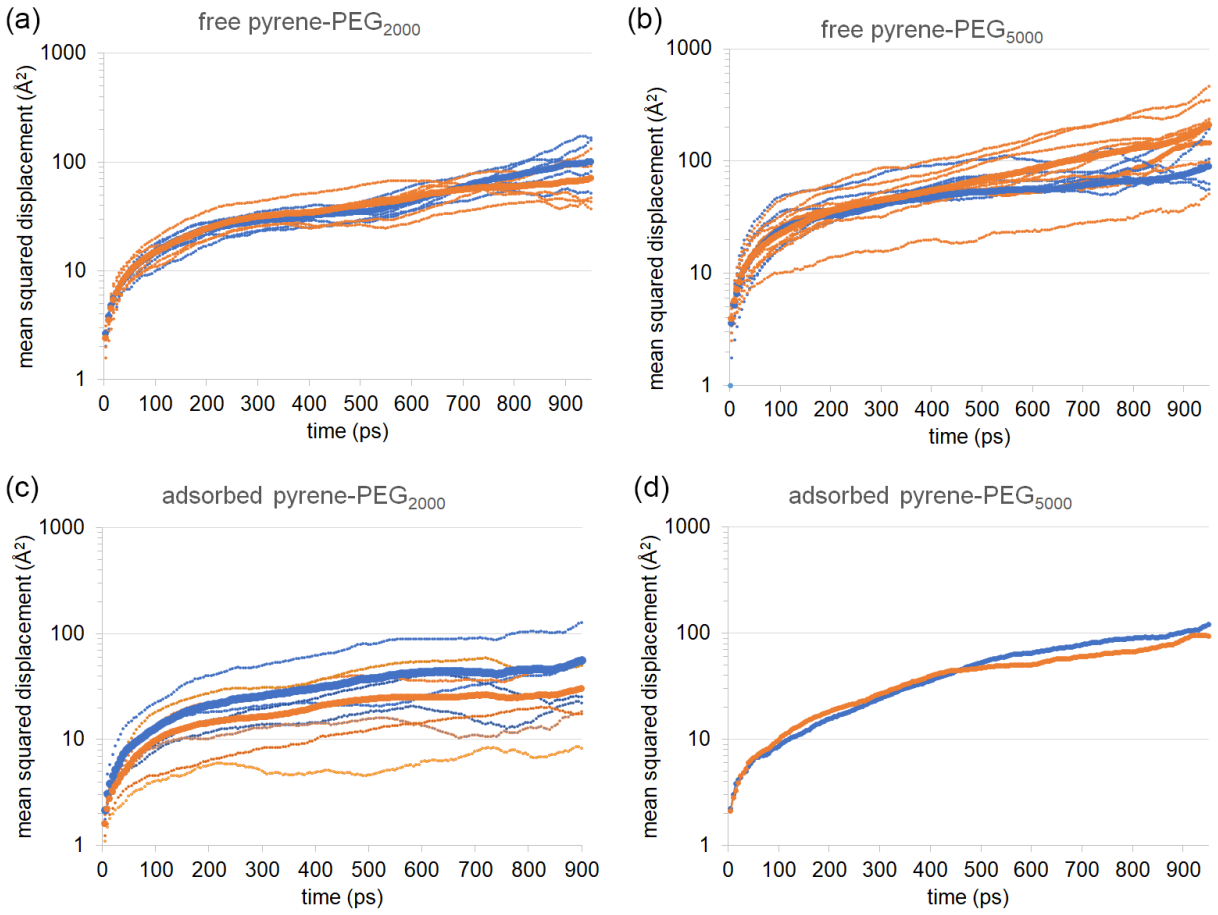

Figure 3. MSD curves of (a) free pyrene-PEG$_{2000}$ chains, (b) free pyrene-PEG$_{5000}$ chains, (c) absorbed pyrene-PEG$_{2000}$ chains, (d) absorbed pyrene-PEG$_{5000}$ chains. Bold curves represent the average MSD values for MD run 1 (blue) and MD run 2 (orange).

2.2. Dynamics of PEG chains

Dynamic behaviors of polymer chains were assessed by average radius of gyration $<R_g>$ and end-to-end distance $<R_e>$. As the number of pyrene ends adsorbed on the SWNT surface was low, PEG chains were considered in the 'mushroom' regime [38]. For both adsorbed and free PEG$_{2000}$ chains, the mean of $<R_g>$ values was calculated as 14.4 Å (Table; Figure 4a). Our results also agreed with the light scattering experiments yielding $R_g = 0.202 \times Mw^{0.550}$ [39], MD simulations with a CHARMM force field [38], and the Gaussian chain model [40] (Table). Differences in the conformational dynamics of adsorbed and free chains were pronounced for PEG$_{5000}$ chains, with a mean of $<R_g>$ values of 18.8 Å and 23.5 Å, respectively (Table; Figure 4b). The main reason for this difference seemed to be the low number of samples for the adsorbed PEG$_{5000}$ chains; this was also reflected in the expected $<R_e>$ value, which will be discussed later. Free PEG$_{5000}$ chains adopted more expanded and compact conformations in the solution, as noted with a wide distribution of R_g values (Figure 4a).

In addition, the distribution of R_g values was obtained for both adsorbed and free chains (Figure 4a). After their pyrene ends adsorbed on the SWNT surface, PEG chains retained their flexibility and they underwent

Table. $<R_e>$ and $<R_g>$ for PEG_{2000} and PEG_{5000} chains.

Chain	$<R_e>$ (Å)					$<R_g>$ (Å)				
	This study: Adsorbed	This study: Free	Ref. [40] : Adsorbed	Ref. [40] : Free	Ref. [38] : Free	This study: Adsorbed	This study: Free	Experiment [39]	Ref. [40]	Ref. [38]
PEG_{2000}	30.1	33.7	28.8	35.0	36.0	14.4	14.4	13.2	14.0	14.5
PEG_{5000}	31.8	58.0	45.5	56.0	56.3	18.8	23.5	21.9	23.0	25.2

different conformations around the nanotube (Figure 4c). For example, the most compact PEG_{2000} chain (adsorbed chain number 8 with $<R_g> \sim 10$ Å in Figure 4a) expanded slightly during the simulations, acquiring a value of 13.0 Å comparable with experimental light scattering data of 13.2 Å. Due to crowding in the system, a few PEG_{2000} chains retained an extended conformation ∼18.0 Å. Similarly, the compact PEG_{5000} chain with a $<R_g>$ of 15.0 Å (Figure 4b, chain number 1) was adsorbed on the SWNT in around 0.5 ns and then maintained its conformation in the crowded medium.

The conformational behavior of adsorbed and free PEG chains was also reflected with the average root mean square end-to-end distance, $<R_e>$ (Figure 4b; Table). After adsorption from the pyrene end, the PEG chain is expected to adopt a $<R_e>$ value slightly larger than $2 \times <R_g>$ in the 'mushroom' regime, according to the Gaussian chain model [40]. In the present study, the $<R_e>$ value averaged for nine adsorbed pyrene-PEG_{2000} chains was 30.1 Å, slightly over 2×14.4 Å, satisfying this theory. With a more focused look, mean R_e values of absorbed and free pyrene-PEG_{2000} chains fluctuated between 15.0 and 50.0 Å.

The $<R_e>$ value averaged for two pyrene-PEG_{5000} chains was lower (31.8 Å) than expected (>45.5 Å) [40] (Table). On the other hand, the $<R_e>$ values of pyrene-PEG_{5000} chains in solution were distributed in a wide range, being between 20.0 and 100.0 Å (Figure 4b). These results reflected the flexibility of long PEG chains, whether adsorbed on the solid surface or freely diffusing in the solution. There was no significant difference between conformational dynamics of the adsorbed and free PEG chains, as expected for the 'mushroom' regime.

2.3. Interaction energy calculations for adsorbed pyrene-PEG on the SWNT

Interaction energies between the pyrene-PEG chains and SWNT were calculated using the trajectory from quench dynamics. The results are displayed in Figure 5. In each simulation, the energy of the first configuration was high, but quickly diminished to an average value. High energies of the first configurations were due to random velocities assigned at the beginning of the simulations. The average interaction energy of the pyrene-PEG_{2000} complex to SWNT was calculated as –71.57 kcal/mol and that of pyrene-PEG_{5000} was –77.59 kcal/mol in water, which were close to each other. These energy values also agreed with our previous findings [32], which indicated interaction energies of –65.99 kcal/mol for pyrene-PEG_{2000} and –72.05 kcal/mol for pyrene-PEG_{5000}. The slight difference between the previous and current results was due to different conformational samplings of the pyrene-PEG chains on the nanotube sidewall.

In the sampling, the pyrene bearing PEG_{5000} started with a perpendicular orientation to the SWNT surface and then changed to a stable parallel conformation. As in MD simulations, while pyrene diffused on the SWNT surface, the flexible PEG chain adopted different conformations, as shown by the lowest energy

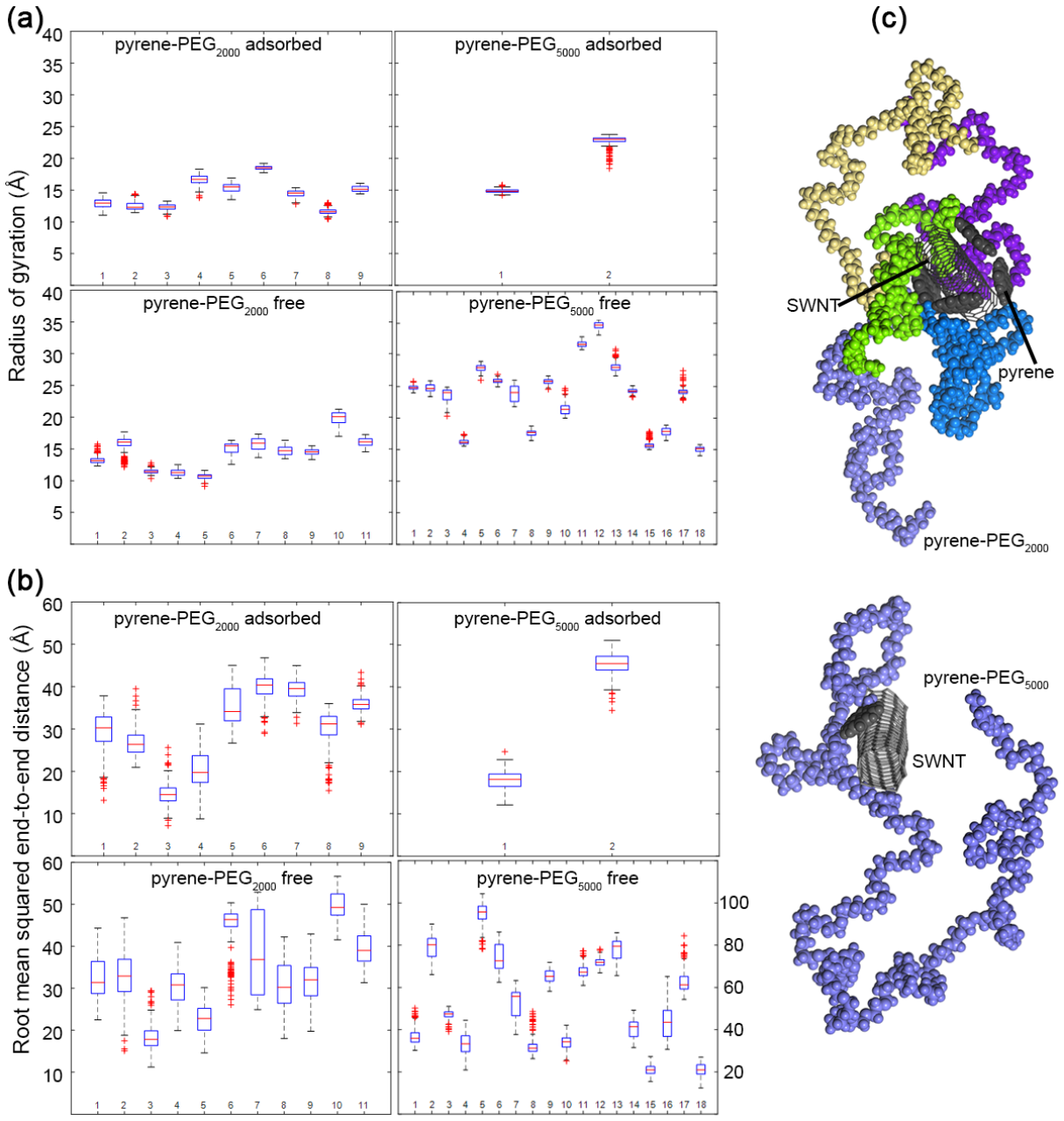

Figure 4. (a) Radius of gyration (R_g), (b) end-to-end distance (R_e) of adsorbed and free PEG chains. (c) Conformations of adsorbed pyrene-PEG chains are shown in different colors. For clarity, water molecules and free chains are hidden.

configurations, indicating the polymer wrapping the SWNT (Figure 5a) and extending to the solvent (Figure 5b).

2.4. Conclusions

Here we reported the details of the early events in adsorption of an aromatic pyrene ring attached to PEG onto a SWNT at atomic level. All-atom MD simulations in water showed that the adsorption of long pyrene-PEG

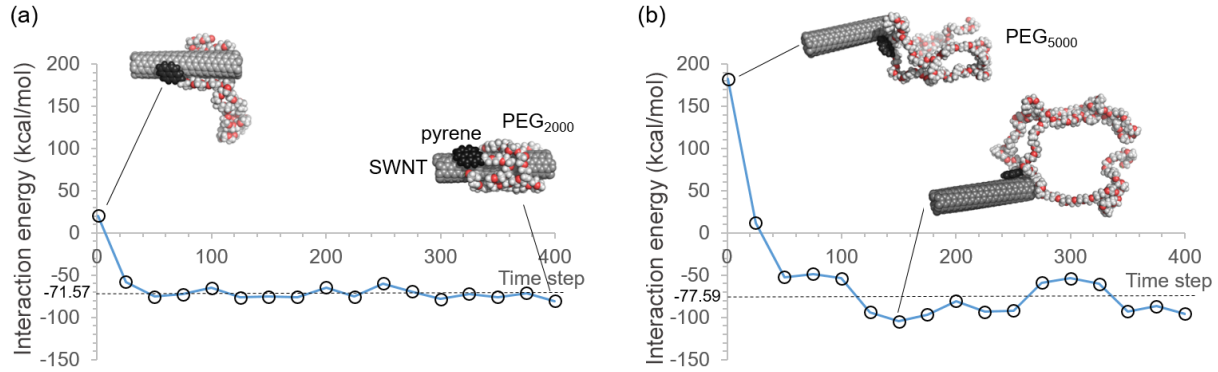

Figure 5. Interaction energy profile for (a) SWNT–pyrene-PEG_{2000} and (b) SWNT–pyrene-PEG_{5000}.

chains from a bulk mixture was driven by the affinity of pyrene to the SWNT surface. Here the effect of PEG molecular weight on stimulating/constraining the diffusion of pyrene ends to the surface seemed to be negligible since the diffusion of PEG chains did not change with respect to molecular weight, as expected for concentrated polymer solutions. On the other hand, the adsorption rate of longer pyrene-polymer chains was lower than that of shorter chains due to steric hindrance on the nanotube surface.

The results also confirmed the stable $\pi - \pi$ stacking interactions between the adsorbed aromatic pyrene molecule and SWNT. Pyrene groups were able to keep their strong interactions with the nanotube, while attached to long and flexible PEG chains, even in different orientations in the concentrated solution. Pyrene-PEG complex could diffuse over the smooth SWNT surface without detaching and a long PEG chain could coat a larger area on the SWNT surface. This observation implied that SWNTs can keep their biocompatibility in blood, which can extend their circulation time with their cargos, such as small drugs.

3. Experimental

The *Build* module of Materials Studio 8.0 was used to generate a single-wall CNT (SWNT) having (6,5) chirality, with diameter 7.0 Å and length 40.0 Å. This diameter was small enough to prevent the diffusion of pyrene-PEG chains inside the nanotube. If the diameter is high enough to allow pyrene-PEG chain diffusion into the nanotube, the fluctuations of the polymer can be hindered in this confined space. This situation was not desired since the dynamic properties of the adsorbed and free chains were aimed to be compared in the present study.

Using the same module, PEG chains with molecular weight 2000 g/mol (PEG_{2000}) and 5000 g/mol (PEG_{5000}) were generated with random conformations; then they were attached to the pyrene molecule from one end. All generated structures were geometrically minimized using the *Smart* method (a cascade of the steepest descent, ABNR, and quasi-Newton methods) of Materials Studio with the COMPASS force field, which is an ab initio force field suitable for organics, inorganics, and polymers to compute their thermophysical properties [41]. An energy convergence criterion of 0.001 kcal/mol was employed to stop the minimization.

The charges of all molecules were calculated using the QEq method [42]. In MD simulation studies, the QEq method is commonly used as a charge equilibration method, depending on ab initio calculations to compute the charges for polymers, ceramics, carbon nanotubes, and biological systems [43,44].

The simulation box of polymeric solution was generated using the *Amorphous Cell* module, where the SWNT and ten copies of pyrene-PEG_{2000} chains were randomly packed. This system was called Model-1. Boxes

were solvated with explicit water, while fixing the density to 1.2 g/cm^3. The system under periodic boundary conditions was minimized, as was explained before, to relax steric clashes that occurred during the packing process. The same procedure was repeated for Model-2 including the SWNT and ten copies of pyrene-PEG$_{5000}$ chains.

MD simulations were carried out using the *Forcite* module with the COMPASS force field. Simulations were run with the canonical ensemble (NVT) at temperature 300 K, which was controlled by a Berendsen thermostat [45] with a decay constant of 0.1 ps. The Ewald summation method was used for electrostatic interactions and a cut-off distance of 12.5 Å was set for long-range interactions. All systems were simulated for 1 ns, which was sufficient to observe the adsorption process of pyrene-PEG chains on SWNTs. A time step of 1 fs was used, and each simulation was repeated twice to obtain independent samples, called MD run 1 and MD run 2.

In addition, a cascade of MD simulations and energy minimization was performed to better sample the configurational space of pyrene-PEG adsorption on the SWNT. Using the *Quench* task of Materials Studio, total MD simulation time was set as 1 ns, where every 100 ps energy minimization was implemented. The same conditions for MD simulations and energy minimization were used as explained before. Then the interaction energy between the pyrene-PEG chain and SWNT was calculated by

$$E_{interaction}=E_{system}-(E_1+E_2), \tag{1}$$

where $E_{interaction}$ was the interaction energy, E_{system} was the total system energy (SWNT and pyrene-PEG), and E_1 and E_2 were the energies of pyrene-PEG chain and SWNT, respectively.

References

1. Comparetti EJ, de Albuquerque Pedrosa V, Kaneno R. Carbon nanotube as a tool for fighting cancer. Bioconjugate Chemistry 2018; 29 (3): 709-718. doi: 10.1021/acs.bioconjchem.7b00563
2. Schroeder V, Savagatrup S, He M, Lin S, Swager TM. Carbon nanotube chemical sensors. Chemical Reviews 2019; 119 (1): 599-663. doi: 10.1021/acs.chemrev.8b00340.
3. Vashist A, Kaushik A, Vashist A, Sagar V, Ghosal A et al. Advances in carbon nanotubes-hydrogel hybrids in nanomedicine for therapeutics. Advanced Healthcare Materials 2018; 7 (9): e1701213. doi: 10.1002/adhm.201701213
4. Son KH, Hong JH, Lee JW. Carbon nanotubes as cancer therapeutic carriers and mediators. International Journal of Nanomedicine 2016; 11: 5163-5185. doi: 10.2147/IJN.S112660.
5. Lee H. Molecular modeling of PEGylated peptides, dendrimers, and single-walled carbon nanotubes for biomedical applications. Polymers 2014; 6 (3): 776-798. doi: 10.3390/polym6030776.
6. Zhou L, Forman HJ, Ge Y, Lunec J. Multi-walled carbon nanotubes: a cytotoxicity study in relation to functionalization, dose, dispersion. Toxicology in Vitro 2017; 42: 292-298. doi: 10.1016/j.tiv.2017.04.027
7. Lee H. Dispersion and bilayer interaction of single-walled carbon nanotubes modulated by covalent and noncovalent PEGylation. Molecular Simulation 2015; 41 (15): 1254-1263. doi: 10.1080/08927022.2014.976638
8. Larson N, Ghandehari H. Polymeric conjugates for drug delivery. Chemistry of Materials 2012; 24 (5): 840-853. doi: 10.1021/cm2031569
9. Jokerst JV, Lobovkina T, Zare RN, Gambhir SS. Nanoparticle PEGylation for imaging and therapy. Nanomedicine 2011; 6 (4): 715-728. doi: 10.2217/nnm.11.19
10. D'souza AA, Shegokar R. Polyethylene glycol (PEG): a versatile polymer for pharmaceutical applications. Expert Opinion on Drug Delivery 2016; 13 (9): 1257-1278. doi: 10.1080/17425247.2016.1182485

11. Al-Qattan M, Deb PK, Tekade RK. Molecular dynamics simulation strategies for designing carbon-nanotube-based targeted drug delivery. Drug Discovery Today 2018; 23 (2): 235-250. doi.org/10.1016/j.drudis.2017.10.002
12. Yang H, Bezugly V, Kunstmann J, Filoramo A, Cuniberti G. Diameter-selective dispersion of carbon nanotubes via polymers: a competition between adsorption and bundling. ACS Nano 2015; 9 (9): 9012-9019. doi: 10.1021/acsnano.5b03051
13. Zheng Q, Xue Q, Yan K, Gao X, Li Q et al. Influence of chirality on the interfacial bonding characteristics of carbon nanotube polymer composites. Journal of Applied Physics 2008; 103: 044302. doi: 10.1063/1.2844289
14. Cai L, Lv W, Zhu H, Xu Q. Molecular dynamics simulation on adsorption of pyrene-polyethylene onto ultrathin single-walled carbon nanotube. Physica E 2016; 81: 226-234. https://doi.org/10.1016/j.physe.2016.03.021
15. Xin X, Xu G, Zhao T, Zhu Y, Shi X et al. Dispersing carbon nanotubes in aqueous solutions by a starlike block copolymer. Journal of Physical Chemistry C 2008; 112 (42): 16377-16384. doi: 10.1021/jp8059344
16. Sarukhanyan E, Milano G, Roccatano D. Coating mechanisms of single-walled carbon nanotube by linear polyether surfactants: insights from computer simulations. Journal of Physical Chemistry C 2014; 118 (31): 18069-18078. doi: 10.1021/jp501559x
17. Eslami H, Behrouz M. Molecular dynamics simulation of a polyamide-66/carbon nanotube nanocomposite. Journal of Physical Chemistry C 2014; 118 (18): 9841-9851. doi: 10.1021/jp501672t
18. Lee H. Molecular dynamics studies of PEGylated single-walled carbon nanotubes: the effect of PEG size and grafting density. Journal of Physical Chemistry C 2013; 117 (49): 26334-26341. doi: 10.1021/jp4093749
19. Tallury SS, Pasquinelli MA. Molecular dynamics simulations of flexible polymer chains wrapping single-walled carbon nanotubes. The Journal of Physical Chemistry B 2010; 114 (12): 4122-4129. doi: 10.1021/jp908001d
20. Fu H, Xu S, Li Y. Nanohelices from planar polymer self-assembled in carbon nanotubes. Scientific Reports 2016; 6: 30310. doi: 10.1038/srep30310
21. Matsuo Y, Tahara K, Nakamura E. Theoretical studies on structures and aromaticity of finite-length armchair carbon nanotubes. Organic Letters 2003; 5 (18): 3181-3184. doi: 10.1021/ol0349514
22. Ormsby JL, King BT. Clar valence bond representation of π-bonding in carbon nanotubes. The Journal of Organic Chemistry 2004; 69 (13): 4287-4291. doi: 10.1021/jo035589+
23. Linert W, Lukovits I. Aromaticity of carbon nanotubes. Journal of Chemical Information and Modeling 2007; 47 (3): 887-890. doi: 10.1021/ci600504r
24. Martin-Martinez FJ, Melchor S, Dobado JA. Edge effects, electronic arrangement, and aromaticity patterns on finite-length carbon nanotubes. Physical Chemistry Chemical Physics 2011; 13: 12844-12857. doi: 10.1039/c1cp20672a
25. Umadevi D, Panigrahi S, Sastry GN. Noncovalent interaction of carbon nanostructures. Accounts of Chemical Research 2014; 47 (8): 2574-2581. doi: 10.1021/ar500168b
26. Zhao YL, Stoddart JF. Noncovalent functionalization of single-walled carbon nanotubes. Accounts of Chemical Research 2009; 42 (8): 1161-1171. doi: 10.1021/ar900056z
27. Perez EM, Martin N. $\pi - \pi$ Interactions in carbon nanostructures. Chemical Society Reviews 2015; 44 (18): 6425-6433. doi: 10.1039/C5CS00578G
28. Gavrel G, Jousselme B, Filoramo A, Campidelli S. Supramolecular chemistry of carbon nanotubes. Topics in Current Chemistry 2014; 348: 95-126. doi: 10.1007/128_2013_450
29. Martin N, Nierengarten JF. Supramolecular Chemistry of Fullerenes and Carbon Nanotubes. Weinheim, Germany: Wiley-VCH, 2012.
30. Calbo J, Lopez-Moreno A, de Juan A, Comer J, Orti E et al. Understanding noncovalent interactions of small molecules with carbon nanotubes. Chemistry A European Journal 2017; 23 (52): 12909-12916. doi: 10.1002/chem.201702756

31. Naotoshi N, Yasuhiko T, Hiroto M. Water-soluble single-walled carbon nanotubes via noncovalent sidewall-functionalization with a pyrene-carrying ammonium ion. Chemistry Letters 2002; 31 (6): 638-639. doi: 10.1246/cl.2002.638
32. Meran M, Akkus PA, Kurkcuoglu O, Baysak E, Hizal G et al. Noncovalent pyrene-polyethylene glycol coatings of carbon nanotubes achieve in vitro biocompatibility. Langmuir 2018; 34 (40): 12071-12082. doi: 10.1021/acs.langmuir.8b00971
33. Chen RJ, Zhang Y, Wang D, Dai H. Noncovalent sidewall functionalization of single-walled carbon nanotubes for protein immobilization. Journal of the American Chemical Society 2001; 123 (16): 3838-3839. doi: 10.1021/ja010172b
34. Bobadilla AD, Samuel EL, Tour J, Seminario J. Calculating the hydrodynamic volume of poly(ethylene oxylated) single-walled carbon nanotubes and hydrophilic carbon clusters. Journal of Physical Chemistry B 2013; 117 (1): 343-354. doi: 10.1021/jp305302y
35. Xu L, Yang X. Molecular dynamics simulation of adsorption of pyrene-polyethylene glycol onto graphene. Journal of Colloid and Interface Science 2014; 418: 66-73. doi: 10.1016/j.jcis.2013.12.005
36. Mosquet M, Chevalier Y, Brunel S, Guicquero JP, Le Perchec P. Polyoxyethylene di-phosphonates as efficient dispersing polymers for aqueous suspensions. Journal of Applied Polymer Science 1997; 65 (12): 2545-2555. doi: 10.1002/(SICI)1097-4628(19970919)65:12<2545::AID-APP24>3.0.CO;2-Y
37. Vrentas JS, Chu CH. Molecular weight dependence of the diffusion coefficient for the polystyrene-toluene system. Journal of Polymer Science Part B: Polymer Physics 1989; 27: 465-468. doi: 10.1002/polb.1989.090270216
38. Lee H, de Vries AH, Marrink SJ, Pastor RW. A coarse-grained model for polyethylene oxide and polyethylene glycol: conformation and hydrodynamics. Journal of Physical Chemistry B 2009; 113 (40): 13186-13194. doi: 10.1021/jp9058966
39. Kawaguchi S, Imai G, Suzuki J, Miyahara A, Kitano T. Aqueous solution properties of oligo- and poly(ethylene oxide) by static light scattering and intrinsic viscosity. Polymer 1997; 38 (12): 2885-2891. doi: 10.1016/S0032-3861(96)00859-2
40. Wang Y, Shu X, Liu J, Ran Q. Conformational properties and the entropic barrier in the "head-on" adsorption of a single polymer chain towards a flat surface. Soft Matter 2018; 14: 2077-2083. doi: 10.1039/c8sm00013a
41. Sun HJ. COMPASS: an ab initio force-field optimized for condensed-phase applications overview with details on alkane and benzene compounds. Journal of Physical Chemistry B 1998; 102 (38): 7338-7364. doi: 10.1021/jp980939v
42. Rappe AK, Goddard III WA. Charge equilibration for molecular dynamics simulations. Journal of Physical Chemistry 1991; 95 (8): 3358-3363. doi: 10.1021/j100161a070
43. Bagri A, Mattevi C, Acik M, Chabal YJ, Chhowalla M et al. Structural evolution during the reduction of chemically derived graphene oxide. Nature Chemistry 2010; 2 (7): 581-587. doi: 10.1038/nchem.686
44. Pupysheva OV, Farajian AA, Knick CR, Zhamu A, Jang BZ. Modeling direct exfoliation of nanoscale graphene platelets. Journal of Physical Chemistry C 2010; 114 (49): 21083-21087. doi: 10.1021/jp1071378
45. Berendsen HJC, Postma JPM, van Gunsteren WF, DiNola A, Haak JR. Molecular-dynamics with coupling to an external bath. Journal of Chemical Physics 1984; 81: 3684. doi: 10.1063/1.448118